Indonesian Journal of Biotechnology

VOLUME 29(1), 2024, 40-47 | RESEARCH ARTICLE

# Detection and quantification of splicing variants of *Hd3a* gene in oil palm

**Aqwin Polosoro[1,2], Wening Enggarini[2], Kusumawaty Kusumanegara[3], Toto Hadiarto[2], Miftahudin[1], Ence Darmo Jaya Supena[1,*]**

[1]Department of Biology, Faculty of Mathematics and Natural Sciences, IPB University, Bogor 16680, Indonesia
[2]Research Center for Genetic Engineering, National Research and Innovation Agency, Bogor 16911, Indonesia
[3]Research Center for Horticulture, National Research and Innovation Agency, Bogor 16911, Indonesia
*Corresponding author: encedarmo@apps.ipb.ac.id

**SUBMITTED** 25 August 2023 **REVISED** 15 January 2024 **ACCEPTED** 23 January 2024

**ABSTRACT** Alternative splicing is a complex process that contributes to the generation of diverse mRNA and protein isoforms, including in oil palm (*Elaeis guineensis*). Despite their importance, many functions of alternative splicing genes remain poorly characterized. This study aims to investigate splicing variants of gene encoding *Heading date 3a* in *E. guineensis* (*EgHd3a*) using the GenBank database and ClustalW algorithm. To ensure the data accuracy and reliability of design isoform-specific primers, special emphasis is given to primer design techniques and validation using polymerase chain reaction (PCR) and quantitative real-time (qRT)-PCR analysis. The designed primers demonstrated high specificity and discrimination between mRNA specimens. Nucleotide variations at the 3'-end influenced the specificity of primers with the addition of GC composition. Furthermore, qRT-PCR analysis revealed a strong correlation between Ct values and gene concentration for the isoforms which indicates a reliable amplification of *EgHd3a*. Although two isoforms, *Hd3a*-X2 and *Hd3a*-X3, showed slightly higher than acceptable PCR efficiency values, caution is advised to prevent non-specific amplification. Despite the challenge posed by the limitation of primer positioning due to alternative splicing, the chosen primer proved optimal for analysis. This study highlights the importance of considering alternative splicing in gene quantification experiments and provides insights into the critical steps, methods, and quality control measures necessary for accurately detecting alternative splicing events, contributing to understanding this complex biological process.

**KEYWORDS** Alternative splicing; *Hd3a*; Primer; mRNA; qRT-PCR

## 1. Introduction

Alternative splicing is a complex process by which a single gene can generate multiple protein isoforms through the inclusion or exclusion of specific combinations of exons in pre-mRNA transcripts (Harvey and Cheng 2016). A large ribonucleoprotein complex, spliceosome, assembles at splice sites and removes introns through a series of phosphodiester transfer events (Fu and Ares 2014). The recognition of splice sites and the branch site, which mark the beginning and end of each intron, is carried out by small nuclear ribonucleoproteins (snRNPs) U1, U2, U4, U5, and U6 (Wilkinson et al. 2020). The spliceosome is one of the most complex machines in the cell that is responsible for removing introns and connecting the chosen exons through two transesterification events (Shang et al. 2017; Szakonyi and Duque 2018). The assembly and regulation of the spliceosome are dynamic processes guided by consensus sequences (Baralle and Giudice 2017).

In plants, alternative splicing occurs to varying degrees, with genome-wide transcriptome mapping revealing ranges from 42% to 61% in *Arabidopsis thaliana* (Klepikova et al. 2016; Shang et al. 2017). Alternative splicing enables the generation of multiple mRNA transcripts from a single pre-mRNA, resulting in increased diversity in the transcriptome and proteome (Yang et al. 2014; Baralle and Giudice 2017; Shang et al. 2017). This process generates novel and unstable mRNA isoforms that are subsequently degraded through nonsense-mediated decay (NMD), contributing to transcript level regulation. Alternative splicing can produce functionally distinct mRNAs encoding protein isoforms with varying subcellular localization, stability, or function, achieved through intron retention, alternative splice site selection, or the presence of premature termination codons (Shang et al. 2017; Szakonyi and Duque 2018).

As a widely cultivated crop, the study on alternative splicing in oil palm has garnered significant interest. Several studies have identified alternative splicing events in oil palm through transcriptome analysis. Zhang et al. (2022) identified 33,434 alternative splicing events in oil palm fruit tissues. One of the genes exhibiting alterna-

tive splicing in oil palm is *Heading date 3a* (*Hd3a*; gene ID: LOC105040685), which is among the most intensively studied types of genes since its importance in plant development (Hassankhah et al. 2020; Li et al. 2015).

Hd3a is a protein that is the homolog of Flowering locus T (FT). It acts as a florigen, which is a key signaling molecule that controls when plants bloom (Purwestri et al. 2012; Tsuji et al. 2015; Yun et al. 2023). Both Hd3a and FT proteins exhibit considerably similar molecular structures and share a common function of inducing flowering (Wu et al. 2019; Polosoro et al. 2021). Given how important FT and Hd3a are to this important biological process, many studies have been done on both of them in different plant species, where it has been found that they both play similar roles in flowering induction (Liu et al. 2016).

Alternative splicing of *Hd3a/FT* has been identified in other species, including in rice (Kaneko-Suzuki et al. 2018), *Platanus acerifolia* (Shao et al. 2022), *Chrysanthemum morifolium* (Mao et al. 2016), and coconut (Xia et al. 2020). This alternative splicing may exert significant effects on plant phenotype. In coconuts, analysis of alternative splicing in photoperiod pathway genes revealed transcript differences between tall and dwarf coconut varieties. Xia et al. (2020) found that the shorter alternative splice variant of the *FT* gene, which has a 6 bp deletion and alternative 3′ splice sites (A3SS), was only found in dwarf coconut varieties and not in most tall coconut varieties. Moreover, alternatively, spliced transcripts help make R proteins that help plants fight off diseases and recognize when pathogens are invading the plants (Yang et al. 2014). However, the major functions of alternative splicing genes remain unknown due to the limitations of the study.

The identification of alternative splicing events in RNA samples is crucial due to their vital function in the biological process. However, the minimal differences in RNA sequences among mRNA isoforms present significant challenges, particularly in quantitative analysis using quantitative real time polymerase chain reaction (qRT-PCR). Therefore, it is essential to develop an accurate and reliable technique to detect alternative splicing. The objectives of this study are to design and validate splicing variant-specific primers for accurately detecting and quantifying the splicing variants of the *EgHd3a* gene, using PCR and qRT-PCR analysis techniques. In this study, we employed the GenBank database built by the National Center for Biotechnology Information (NCBI) and the ClustalW algorithm suite to find alternative splicing events and visualize genomic DNA and mRNA samples. We prioritized good primer design and primer validation utilizing PCR and qRT-PCR analyses for accurate and reliable data. This study also covers the methods, and quality control measures needed to detect alternative splicing events in gene quantification, which can help us understand the complicated mechanics of alternative splicing in biological systems. The complexity of alternative splicing in oil palm and its critical role in gene regulation and trait diversity can be elucidated. Understanding these patterns is pivotal for developing superior varieties with enhanced disease resistance, yield, and environmental adaptability.

## 2. Materials and Methods

### 2.1. Alternative splicing identification

The genomic sequence of *Hd3a* gene in oil palm and mRNA samples were obtained from NCBI database based on previous study conducted by Polosoro et al. (2021) and Whankaew et al. (2019). Alternative splicing was visualized by comparing genomic DNA and mRNA using the ClustalW method (Supplementary data 1).

### 2.2. Alternative splicing visualization and primer design

To visualize the alternative splicing, forward and reverse primer pairs were designed manually at unique/specific target sequences to generate 70–150 bp amplicon with low secondary structure (GC content <60%). The primer design followed established guidelines, including a length of 15–20 bp, a GC content of approximately 50–55%, and a melting temperature of 65 °C, which is approximately 5 °C higher than the annealing temperature (60 °C). The primers were anchored with a G/C at the 3'-end and had similar annealing/extension temperatures. To ensure the absence of primer dimer formation, we assessed the probability of dimer formation using the Multiple Primer Analyzer tool by ThermoFisher Scientifc (ThermoFisher Scientific, NA).

### 2.3. Primer validation

To examine primer specificity, especially for mRNA specimens of similar sizes, cloning of the mRNA samples into a vector was performed. Total RNA was extracted from whole oil palm mature male flowers using a modified RNeasy kit (QIAGEN, USA) (Polosoro et al. 2024). The flowers were collected from the 17$^{th}$ frond position, which has commonly reached the stage of anthesis for our oil palm. Total cDNA was made using the ReverTra Ace™ reverse transcriptase kit (Toyobo, Japan). All EgHd3a variant fragments were amplified using MyTaq™ DNA Polymerase (Bioline, USA) and primers flanking the *EgHd3a* gene (F: GCAGATCTATGAGCAGAGAAAGGGATCC and R: CTGGTACCTTAAGGTTGCATCCTTCTCC) with standard recommended procedure. The amplification process of the gene fragment was performed on a PCR thermal cycler (Bio-Rad, USA) with the following cycle: a denaturation stage at 95 °C for 20 s, primer annealing at 60 °C for 30 s, and DNA elongation at 72 °C for 35 s. This PCR cycle was repeated 35 times and concluded with a final elongation stage at 72 °C for 2 min. The resulting amplifications were ligated into pTA cloning vectors (Toyobo, Japan) and transformed into competent *E. coli* strain DH5α cells. Positive clones were identified by direct PCR using gene-clamping primers. Subsequently, 50 colonies were selected, cultured in liquid media, and plasmid extraction was performed using the QIAprep Spin Miniprep Kit (QIAGEN, USA). Finally, specific

primers were used to confirm the presence of the target sequence in all plasmids (Table 1).

**TABLE 1** List of specific primer sequence generated from alternative splicing analysis of *EgHd3a* gene.

| No | Primer Name | Primer Sequences |
|---|---|---|
| 1 | F_EgHd3aX1 | ACCTTCTACACCCTTGGTGTCC |
| | R_EgHd3aX1 | CACACAATCTCCTGACCGTAG |
| 2 | F_EgHd3aX2 | GGACCTTCTACACCCTTATTATG |
| | R_EgHd3aX2 | CACACAATCTCCTGACCGTAG |
| 3 | F_EgHd3aX3 | GGACCTTCTACACCCTTATTATG |
| | R_EgHd3aX3 | CACACAATCTCCTGACCTGAAC |

The primer specificity was further confirmed by performing qRT-PCR. All cloned plasmids underwent a serial dilution, with each being diluted 10 times to create 5 standard samples. Each sample was mixed with 12.5 µL of SensiFAST™ SYBR® No-ROX Kit (Bioline, USA) containing SYBR® Green dye, 0.75 µL of forward and reverse primers (10 mM), 1 µL of plasmid dilution product, and dd$H_2O$ to achieve a total reaction volume of 25 µL. The PCR reaction was performed on a Rotor-Gene Q real-time PCR cycler (QIAGEN, USA) using the absolute quantification mode with three replications. The reaction consisted of an initial denaturation step of 2 min at 95 °C. However, due to the failure to obtain X3 mRNA specimens, cDNA samples with 2× serial dilutions were used instead. Standard curves were analyzed with the Rotor-Gene Q series software (QIAGEN, USA), following recommended procedural guidelines. Melting point data for the three types of amplicons were collected and subsequently analyzed using Duncan's multiple-range test, utilizing SAS software (SAS Institute Inc., USA).

## 3. Results and Discussion

*EgHd3a* gene is located on chromosome 3 of the oil palm genome and produces three distinct protein isoforms: XP_029119083.1, XP_019705100.1, and XP_019705101.1, as documented by Whankaew et al. (2019). These isoforms correspond to three different mRNA sequences, namely XM_019849541.2, XM_019849542.2, and XM_029263250.1, which were designated as specimens X1, X2, and X3, respectively. Among these isoforms, X2 mRNA demonstrates protein homology with the Hd3a and FT proteins (Polosoro et al. 2021). However, it shares common exons with the other isoforms, except for the second exon in X1 mRNA and the fourth exon in X3 mRNA. Notably, the fourth exon in X3 mRNA exhibits a longer exon and a premature stop codon (Figure 1), resulting in a smaller protein and a significant alteration in the protein structure. In comparison, X1 mRNA possesses a second exon that is 24 bases longer than X2, which suggests the presence of an additional 8 amino acids within the Hd3a-like protein structure. These findings emphasize the variation among the isoforms, with X2 mRNA demonstrating similarities with Hd3a and FT proteins, while X1 mRNA exhibits a longer second exon and potential amino acid variations, and X3 mRNA undergoes significant changes in protein structure due to a shorter protein length and possible loss of specific domains.

Using multiple alignment data, the sequences were found in different among mRNA samples. The precise positions of the primers are depicted in Figure 2. For X1, the forward primer is situated on the second exon and has a specific sequence encompassing an additional 24 bases. In contrast, the forward primers for X2 and X3 are identical and located on the first exon, extending five bases into the second exon. The reverse primers for X1 and X2 are derived from the end of the third exon, with an additional 16 bases from the beginning of the fourth exon. Conversely, the reverse primer for X3 corresponds to a sequence that is unique to this particular mRNA specimen (Figure 2).

Primer design is a crucial step in ensuring the specificity and efficiency of PCR amplification. Several factors that influence primer design are the length and complexity of the target sequence, the presence of single nucleotide polymorphisms (SNPs) or insertions/deletions (indels), and the intended application (Kalendar et al. 2022). To achieve specific binding to the template DNA, it is essential to select a stable and specific 3′-end. Regions of the template that contain repetitive sequences or exhibit high similarity to other sequences in the genome should be avoided. High guanine-cytosine (GC) content at the 3′-end of a primer can lead to non-specific binding. In this study, the 3′-end of the primer was selected from the al-

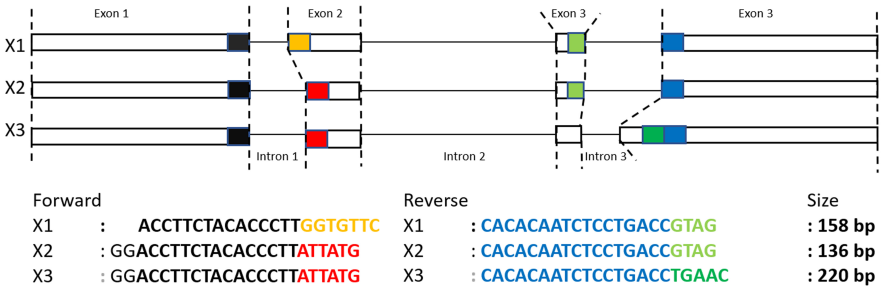


**FIGURE 1** Simplified illustration of unspliced mRNA precursor with four exons (1, 2, 3, and 4) and three introns (shown as lines). Specific primer positions within the exon were shown as blocked boxes and their sequences were indicated with the same color.

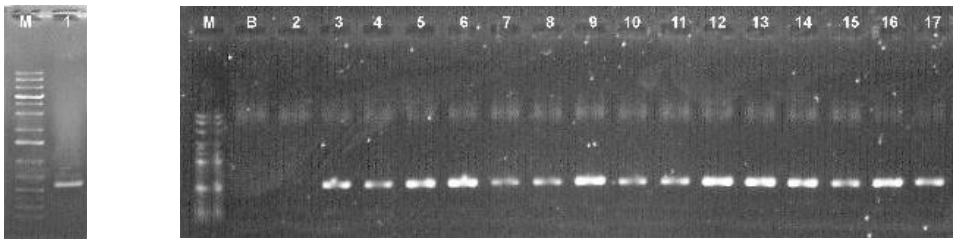


**FIGURE 2** PCR amplicon product from (a) mature male flower cDNA using *EgHd3a* flanking primer (X1 and X2 at around 550 bp and X3 at 654bp) and (b) direct PCR from *E. coli* colony from cloning result, every electrophoresis hole related to one colony. M= 1 kb plus DNA marker, B=blank, 1 = PCR result of cDNA sample, 1-17 = results of direct PCR from colony samples.

ternatively spliced region to enhance the specificity of the target sequence. A range of annealing temperatures was used to ensure specific binding during PCR. Careful evaluation and design of the 3′-end of the primer are crucial for achieving efficient and specific PCR amplification.

In this study, we assessed primer specificity by insertion of the mRNA specimens into the pTA cloning vector. While we successfully cloned two mRNA specimens, the X3 specimen proved to be challenging due to its significantly low expression level (Figure 2a). To gain further insights to this matter, we conducted direct PCR cloning on 50 colonies. Surprisingly, all the colonies showed a band of approximately 550 bp (Figure 2b). Subsequent sequencing analysis confirmed that these colonies exclusively contained cDNA specimens for X1 and X2. Notably, the cDNA and colony amplification approaches failed to detect the presence of the X3 specimen, indicating an extremely low expression level.

The results of PCR using the specific primers demonstrated excellent discrimination between the three mRNA specimens. Primer pair X1 exhibited specific amplification with the X1 specimen at the lowest annealing temperature of 55 °C, as evidenced by the absence of a band on the X2 specimen (Figure 3a). Conversely, primer pair X2 amplified the X1 specimen at annealing temperatures of 55 °C and 58 °C but achieved specificity at a higher

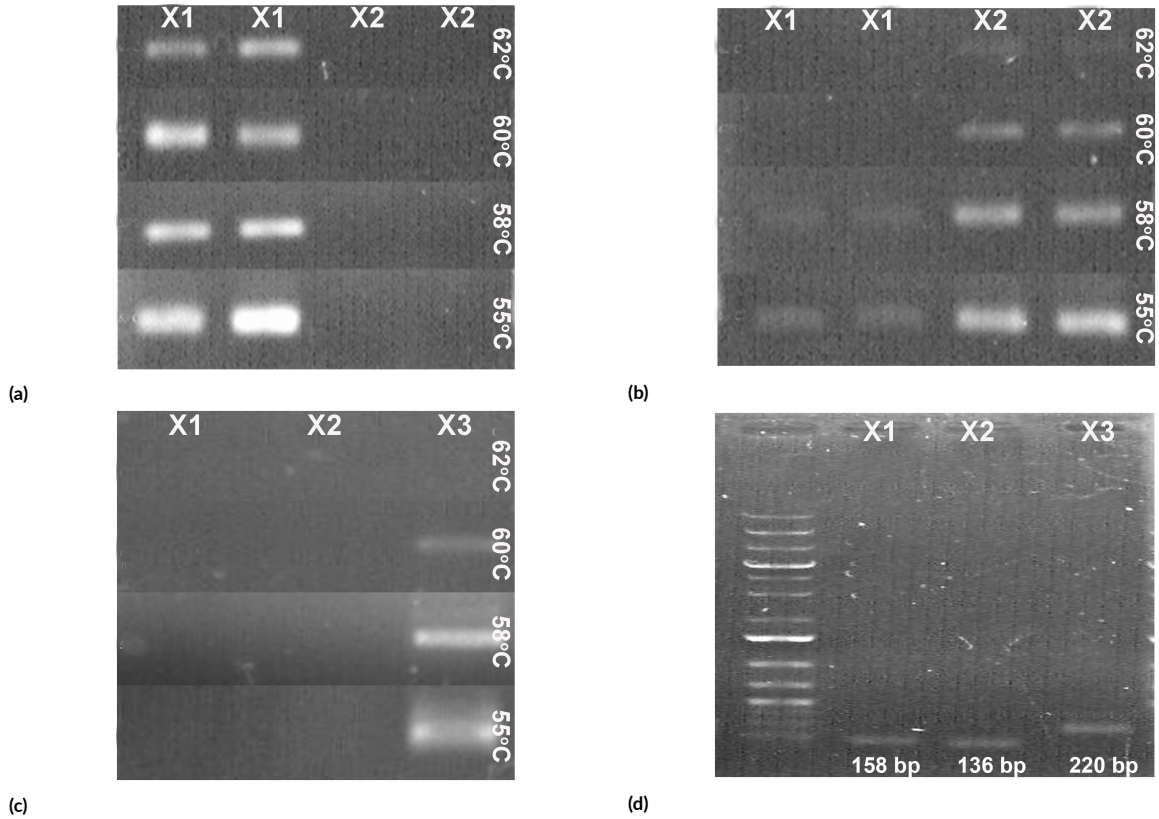


**FIGURE 3** PCR optimization for amplification of three mRNA specimens with X1, X2, and X3 specific primers at different annealing temperatures. (a) Amplification of X1 and X2 cloned fragment using X1 specific primer. (b) Amplification of X1 and X2 cloned fragment using X2 specific primer. (c) Amplification of X1 fragment, X2 fragment, and cDNA using X3 specific primer. (d) Amplification of cDNA using X1, X2, and X3 specific fragment. M= 1 kb plus DNA marker, X1= EgHd3a-X1 (158 bp), X2 = EgHd3a-X2 (136 bp), and X3 = EgHd3a-X3 (220 bp).

annealing temperature of 60 °C (Figure 3b). On the other hand, primer pair X3 exhibited strong specificity at low annealing temperatures (Figure 3d). Importantly, the specificity of this primer pair was observed in cDNA samples annealed at 60 °C, as seen in Figure 3d, where all samples showed a single band.

In the case of SNAP primer design, the 3′-end of a primer plays a crucial role in the successful amplification of the target gene. It is essential to design the primer with a 3′-end that specifically binds to the target sequence and allows for efficient elongation during PCR (Busk 2014). Additionally, incorporating three GC nucleotide bases at the last five bases at the 3′-end can prevent secondary formations, that may interfere with amplification efficiency (Li et al. 2020; Mardalisa et al. 2021). A well-designed primer with a stable and specific 3′-end can significantly enhance the specificity and sensitivity amplification (Pal 2022).

Primer forward X1 exhibits notable differences in the last 7 bases when compared to specimens X2/X3. It contains two bases capable of forming T-A bonds and two C bases in the last 5 bases at the 3′-end (Figure 4a). Despite the presence of T-A bonds, the 7-nucleotide disparity at the 3′-end of primer X1 confers a high level of specificity. In contrast, primer forward X2/X3 has six nucleotide bases that are different from X1 at the 3′-end, with one T-A bond and only one G base in the last five bases (Figure 4b). However, PCR test results indicate that this primer is still capable of amplifying specimen X1 at annealing temperatures below 60 °C (Figure 2b). This suggests that the impact of the T-A bonds on specificity appears to be relatively weak, while the presence of GC bases improves specificity.

Similar effects of GC content on primer specificity are observed in the reverse primers. Five nucleotide bases at the 3′-end of the reverse X1/X2 primer are different from the X3 sequence. There is one T-A bond and three GC bases in the last five bases (Figure 4c). Similar to primer forward X1, this reverse primer also demonstrates a high level of specificity. Additionally, primer reverse X3 has five different bases at the 3′-end compared to the X1/X2 sequence, with two GC bases in the last five bases and no nucleotide bases binding (Figure 4d). It also exhibits high levels of specificity. The presence of G or C bases within the last five bases at the 3′-end of the primer, known as the GC clamp, facilitates a more specific binding affinity at the 3′-end due to the increased stability of G-C base pairing.

However, caution must be exercised to avoid including more than three consecutive G or C bases within the last five bases at the 3′-end of the primer to ensure optimal primer specificity (Jadav et al. 2016). Understanding these factors can help enhance the accuracy and efficiency of PCR-based experiments.

As a confirmation of what was found with traditional PCR, a melting point analysis based on qRT-PCR (Table 2) was conducted to verify the identity of the amplified products. The analysis confirmed that each PCR amplicon originated from a single mRNA specimen. The X1 specimen displayed a distinct peak at 84.17 °C, the X2 specimen exhibited a peak at 84.92 °C, and the X3 specimen showed a peak at 84.46 °C. These melting points were significantly different from each other, indicating that the designed primers were highly specific to their target mRNA samples and could distinguish closely related sequences. Melting point analysis is widely used in research and clinical settings for SNP genotyping in various organisms (Li et al. 2014).

Using qRT-PCR analysis, the *EgHd3a*-X1, *EgHd3a*-X2, and *EgHd3a*-X3 primers exhibited a strong positive linear relationship with correlation coefficients of 99.88%, 99.34%, and 99.12%, respectively (Table 2). These high correlation coefficients indicate a tight relationship be-

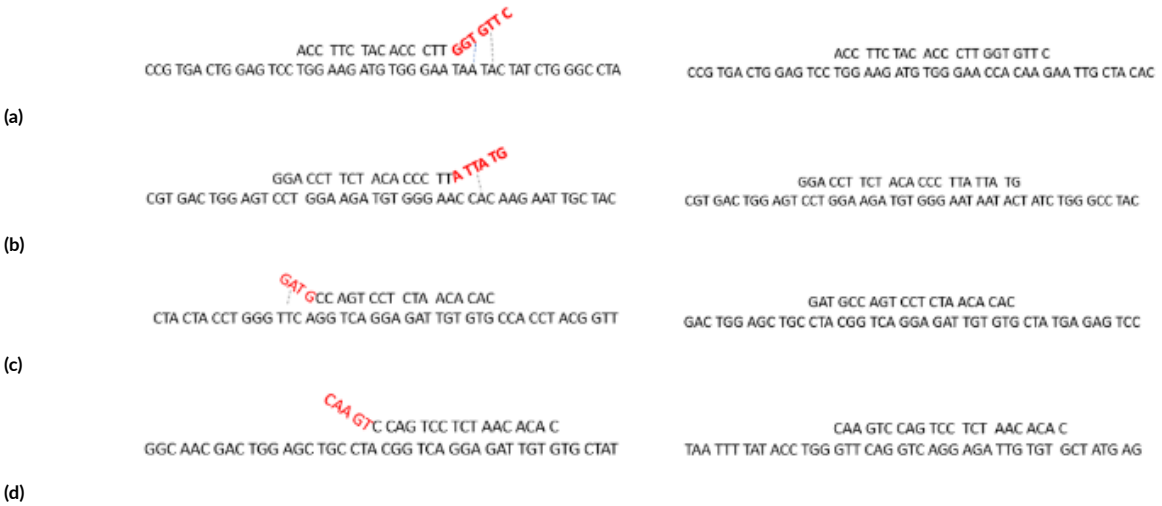


**FIGURE 4** Attachment location of primer (a) forward *EgHd3a*-X1 in the sequence *EgHd3a*-X2/*EgHd3a*-X3 (left) and *EgHd3a*-X1 (right), (b) forward *EgHd3a*-X2/ *EgHd3a*-X3 in the sequence *EgHd3a*-X1(left) and *EgHd3a*-X2 (right), (c) reverse *EgHd3a*-X1/*EgHd3a*-X2 in the sequence *EgHd3a*-X3 (left) and *EgHd3a*-X1/*EgHd3a*-X2 (right), and (d) reverse *EgHd3a*-X3 in the sequence *EgHd3a*-X1/*EgHd3a*-X2 (left) and *EgHd3a*-X3 (right). The red sequences indicate un-attached sequence to template.

**TABLE 2** List of specific primer sequence generated from alternative splicing analysis of *EgHd3a* gene.

| Primer | Regression | R2 | PCR Efficiency | Amplicon Tm |
|---|---|---|---|---|
| *EgHd3aX1* | 99.89% | 0.99774 | 110% | 84.17°C *a |
| *EgHd3aX2* | 99.34% | 0.98688 | 116% | 84.91°C *c |
| *EgHd3aX3* | 99.12% | 0.96247 | 115% | 84.46°C *b |

*a, b, and c denote statistical significance

tween Ct values and the logarithm of the mRNA specimens' concentration (Supplementary data 2). The standard curve in qRT-PCR is a crucial component that enables accurate quantification of DNA fragments (Adams 2020). By establishing a correlation between the Ct values (cycle threshold) and the logarithm of the target gene's concentration, the standard curve allows researchers to estimate the gene's concentration in unknown samples with precision and reliability (Bak and Emerson 2019; Adams 2020).

The efficiency of a PCR reaction is a critical parameter that directly influences the accuracy and reliability of gene expression quantification. Typically, the acceptable and desirable range for PCR efficiency is between 90% and 110% for most experiments (Tellinghuisen and Spiess 2015). Based on the analysis presented in Figure 4, the qRT-PCR standard curve analysis demonstrates that the amplification processes for all three mRNA specimens are generally efficient. *EgHd3a*-X1 mRNA showed an efficiency within the acceptable range, indicating optimal amplification. According to Svec et al. (2015), when the efficiency falls within this range, the amplification process is reliable and effective, allowing for accurate measurement of gene expression levels. Maintaining optimal efficiency is crucial as it ensures consistent amplification of the target gene at the expected rate. Several factors, including primer design, template purity, PCR reagent, and thermal cycler conditions, can contribute to fluctuations in efficiency (Bustin and Huggett 2017).

Conversely, the efficiency values of *EgHd3a*-X2 and *EgHd3a*-X3 primers exceed the upper limit, suggesting the possibility of more efficient amplification. While higher efficiency values can increase the assay's sensitivity, caution must be exercised due to the risk of non-specific amplification or other errors (Zuhar 2019). Therefore, meticulous optimization of experimental conditions is essential to achieve efficiency within the normal range, ensuring precise and reliable quantification of gene expression levels. In this case, where alternative splicing limits primer positioning options, it is important to note that the selected primer remains the optimal choice for analysis. By carefully considering efficiency values and making appropriate experimental adjustments, an accurate and meaningful interpretation of the qRT-PCR results can be achieved.

## 4. Conclusions

In conclusion, our study focused on the *EgHd3a* gene and its mRNA isoforms in oil palm to design primers for accurately detecting and quantifying the splicing variants of the *EgHd3a* gene. Our analysis showed that the designed primers were highly specific and capable of differentiating between mRNA samples. Notably, the variations in nucleotides at the 3'-end of the primers, particularly the GC composition, played a crucial role in enhancing the specificity of primers.

The analysis of the qRT-PCR standard curve demonstrated a strong correlation between Ct values and gene concentration for the *EgHd3a*-X1, *EgHd3a*-X2, and *EgHd3a*-X3 primers. While *EgHd3a*-X1 primer demonstrated efficiency values within an acceptable range, caution was advised for *EgHd3a*-X2 and *EgHd3a*-X3 primers, as their slightly higher efficiency values necessitate meticulous optimization to prevent potential non-specific amplification. Despite encountering challenges with primer positioning due to alternative splicing, our chosen primer proved to be optimal for the comprehensive analysis conducted in this study. Overall, our research emphasizes the importance of considering alternative splicing in gene quantification experiments. It provides valuable insights into methodologies and quality control measures, ensuring precise and accurate detection of alternative splicing events. However, this research may not be applicable in the case of very high or very low GC content and highly repeat area of adjacent splicing area. Future research including the transformation of specimens to model plants and its quantification in different populations may confirm the function of this alternative splicing. The findings presented in this study significantly contribute to the understanding of gene expression dynamics in oil palm and open avenues for further advancements in molecular studies and genetic research in plant species.

## Acknowledgments

The authors extend their sincere gratitude to the National Research and Innovation Agency for their invaluable support in providing the necessary research facilities for the successful completion of this study. Their commitment to advancing scientific research and promoting innovation has been instrumental in facilitating our investigations.

## Authors' contributions

AP, TH, M, EDJS designed the study. AP carried out the laboratory work. AP, TH analyzed the data. AP, WE, KK, TH, M, EDJS wrote the manuscript. All authors read and approved the final version of the manuscript.

## Competing interests

The authors declare no competing interest.

## References


Adams G. 2020. A beginner's guide to RT-PCR, qPCR and RT-qPCR. Biochem. (Lond). 42(3):48–53. doi:10.1042/bio20200034.

Bak A, Emerson JB. 2019. Multiplex quantitative PCR for single-reaction genetically modified (GM) plant detection and identification of false-positive GM plants linked to Cauliflower mosaic virus (CaMV) infection. BMC Biotechnol. 19(1):1–12. doi:10.1186/s12896-019-0571-1.

Baralle FE, Giudice J. 2017. Alternative splicing as a regulator of development and tissue identity. Nat. Rev. Mol. Cell Biol. 18(7):437–451. doi:10.1038/nrm.2017.27.

Busk PK. 2014. A tool for design of primers for microRNA-specific quantitative RT-qPCR. BMC Bioinformatics 15(1):29. doi:10.1186/1471-2105-15-29.

Bustin S, Huggett J. 2017. qPCR primer design revisited. Biomol. Detect. Quantif. 14:19–28. doi:10.1016/j.bdq.2017.11.001.

Fu XD, Ares M. 2014. Context-dependent control of alternative splicing by RNA-binding proteins. Nat. Rev. Genet. 15(10):689–701. doi:10.1038/nrg3778.

Harvey SE, Cheng C. 2016. Methods for characterization of alternative RNA splicing. Methods Mol. Biol. 1402:229–241. doi:10.1007/978-1-4939-3378-5_18.

Hassankhah A, Rahemi M, Ramshini H, Sarikhani S, Vahdati K. 2020. Flowering in Persian walnut: Patterns of gene expression during flower development. BMC Plant Biol. 20(1):1–10. doi:10.1186/s12870-020-02372-w.

Jadav KK, Rajput N, Singh AP, Sarkhel BC, Shrivastav AB. 2016. A species-specific ARMS PCR test for detection of Indian wild pig DNA. Indian J. Anim. Sci. 86(6):67–70. URL https://www.researchgate.net/publication/323355376.

Kalendar R, Shustov AV, Akhmetollayev I, Kairov U. 2022. Designing allele-specific competitive-extension PCR-based assays for high-throughput genotyping and gene characterization. Front. Mol. Biosci. 9:1–13. doi:10.3389/fmolb.2022.773956.

Kaneko-Suzuki M, Kurihara-Ishikawa R, Okushita-Terakawa C, Kojima C, Nagano-Fujiwara M, Ohki I, Tsuji H, Shimamoto K, Taoka KI. 2018. TFL1-like proteins in rice antagonize rice FT-like protein in inflorescence development by competition for complex formation with 14-3-3 and FD. Plant Cell Physiol. 59(3):458–468. doi:10.1093/pcp/pcy021.

Klepikova AV, Kasianov AS, Gerasimov ES, Logacheva MD, Penin AA. 2016. A high resolution map of the *Arabidopsis thaliana* developmental transcriptome based on RNA-seq profiling. Plant J. 88(6):1058–1070. doi:10.1111/tpj.13312.

Li C, Zhang Y, Zhang K, Guo D, Cui B, Wang X, Huang X. 2015. Promoting flowering, lateral shoot outgrowth, leaf development, and flower abscission in tobacco plants overexpressing cotton *FLOWERING LOCUS T* (*FT*)-like gene *GhFT1*. Front. Plant Sci. 6(June):1–14. doi:10.3389/fpls.2015.00454.

Li D, Zhang J, Li J. 2020. Primer design for quantitative real-time PCR for the emerging Coronavirus SARS-CoV-2. Theranostics 10(16):7150–7162. doi:10.7150/thno.47649.

Li KC, Ding ST, Lin EC, Wang L, Lu YW. 2014. Melting analysis on microbeads in rapid temperature-gradient inside microchannels for single nucleotide polymorphisms detection. Biomicrofluidics 8(6):1–15. doi:10.1063/1.4902907.

Liu YY, Yang KZ, Wei XX, Wang XQ. 2016. Revisiting the phosphatidylethanolamine-binding protein (PEBP) gene family reveals cryptic *FLOWERING LOCUS T* gene homologs in gymnosperms and sheds new light on functional evolution. New Phytol. 212(3):730–744. doi:10.1111/nph.14066.

Mao Y, Sun J, Cao P, Zhang R, Fu Q, Chen S, Chen F, Jiang J. 2016. Functional analysis of alternative splicing of the *FLOWERING LOCUS T* orthologous gene in *Chrysanthemum morifolium*. Hortic. Res. 3:16058. doi:10.1038/hortres.2016.58.

Mardalisa, Suhandono S, Yanti N, Rozi F, Nova F, Primawati. 2021. Bioinformatic analysis in designing mega-primer in overlap extension PCR cloning (OEPC) technique. Int. J. Informatics Vis. 5(2):139–143. doi:10.30630/joiv.5.2.459.

Pal A. 2022. Rapid amplification of cDNA ends (RACE). Protoc. Adv. Genomics Allied Tech. p. 505–535. doi:10.1007/978-1-0716-1818-9_21.

Polosoro A, Enggarini W, Hadiarto T, Miftahudin, Supena EDJ. 2024. Optimizing RNA extraction and cloning techniques: a case study of cloning the *Heading date 3a* gene in oil palm [manuscript submitted for publication]. Ph.D. thesis, Departement of Plant Biology, IPB University, Bogor.

Polosoro A, Enggarini W, Hadiarto T, Supena ED, Suharsono. 2021. In silico screening of oil palm early and continuously flowering gene candidates for faster breeding program. In: IOP Conf. Ser. Earth Environ. Sci., volume 762. p. 012063. doi:10.1088/1755-1315/762/1/012063.

Purwestri YA, Ogaki Y, Tsuji H, Shimamoto K. 2012. Functional analysis of *OsKANADI1*, a florigen *Hd3a* interacting protein in rice (*Oryza sativa* L.). Indones. J. Biotechnol. 17(2):169–176. doi:10.22146/ijbiotech.7860.

Shang X, Cao Y, Ma L. 2017. Alternative splicing in plant genes: A means of regulating the environmental fitness of plants. Int. J. Mol. Sci. 18(2):1–18. doi:10.3390/ijms18020432.

Shao C, Cai F, Zhang Y, Bao Z, Shi G, Bao M, Zhang J. 2022. Regulation of alternative splicing of *PaFT* and *PaFDL1*, the *FT* and *FD* homologs in *Platanus acerifolia*. Gene 830:146506. doi:10.1016/j.gene.2022.146506.

Svec D, Tichopad A, Novosadova V, Pfaffl MW, Kubista

M. 2015. How good is a PCR efficiency estimate: Recommendations for precise and robust qPCR efficiency assessments. Biomol. Detect. Quantif. 3:9–16. doi:10.1016/j.bdq.2015.01.005.

Szakonyi D, Duque P. 2018. Alternative splicing as a regulator of early plant development. Front. Plant Sci. 9:1–9. doi:10.3389/fpls.2018.01174.

Tellinghuisen J, Spiess AN. 2015. Bias and imprecision in analysis of real-time quantitative polymerase chain reaction data. Anal. Chem. 87(17):8925–8931. doi:10.1021/acs.analchem.5b02057.

Tsuji H, Tachibana C, Tamaki S, Taoka KI, Kyozuka J, Shimamoto K. 2015. Hd3a promotes lateral branching in rice. Plant J. 82(2):256–266. doi:10.1111/tpj.12811.

Whankaew S, Ruttajorn K, Madsen CK, Asp T, Xu L, Nakkaew A, Phongdara A. 2019. An *EgHd3a-like* and its alternatively spliced transcripts in the oil palm (*Elaeis guineensis*). Songklanakarin J. Sci. Technol. 41(2):332–340. doi:10.14456/sjst-psu.2019.42.

Wilkinson ME, Charenton C, Nagai K. 2020. RNA Splicing by the Spliceosome. Annu. Rev. Biochem. 89:359–388. doi:10.1146/annurev-biochem-091719-064225.

Wu Y, Wei J, Choi SC, Fei Y, Xiong F. 2019. Rice florigen gene Hd3a has conserved functions in callus development. Acta Physiol. Plant. 41(7):125. doi:10.1007/s11738-019-2914-x.

Xia W, Liu R, Zhang J, Mason AS, Li Z, Gong S, Zhong Y, Dou Y, Sun X, Fan H, Xiao Y. 2020. Alternative splicing of flowering time gene *FT* is associated with halving of time to flowering in coconut. Sci. Rep. 10(1):1–11. doi:10.1038/s41598-020-68431-2.

Yang S, Tang F, Zhu H. 2014. Alternative splicing in plant immunity. Int. J. Mol. Sci. 15(6):10424–10445. doi:10.3390/ijms150610424.

Yun HR, Chen C, Kim JH, Kim HE, Karthik S, Kim HJ, Chung YS, Baek HS, Sung S, Kim HU, Heo JB. 2023. Genome-edited *HEADING DATE 3a* knockout enhances leaf production in *Perilla frutescens*. Front. Plant Sci. 14:1–12. doi:10.3389/fpls.2023.1133518.

Zhang A, Jin L, Yarra R, Cao H, Chen P, John Martin JJ. 2022. Transcriptome analysis reveals key developmental and metabolic regulatory aspects of oil palm (*Elaeis guineensis* Jacq.) during zygotic embryo development. BMC Plant Biol. 22(1):1–13. doi:10.1186/s12870-022-03459-2.

Zuhar LM. 2019. Determination of reference genes for normalisation of gene expression study of *Ganoderma*-infected oil palms. J. Oil Palm Res. 31(4):550–560. doi:10.21894/jopr.2019.0051.